A Novel Regiospecific Intramolecular Cycloaddition of an Aromatic Ring. Molecular Orbital Study of Conjugated Ketenes Thermally Generated from Six-membered α-Monocarbonyl Azo-compounds

Masayuki Kuzuya,* Fumio Miyake, and Takachiyo Okuda
Gifu College of Pharmacy, 6–1 Mitahora-higashi 5-Chome, Gifu 502, Japan

When a methylene dichloride solution containing 4,4-diarylphthalazin-1(4*H*)-one (**3**) was warmed above −50 °C, nitrogen extrusion occurred to result in the formation of the quinonoid ketene (**19**). The quinonoid ketene thus generated underwent a facile and regiospecific intramolecular [$_{\pi}4_a + {}_{\pi}2_a$] cycloaddition with *NN*-dimethylaniline to afford a norcaradiene (**22**), followed by ring opening to an azulenone derivative (**14**). It was found, however, that this process takes place only with an aromatic ring bearing strong electron-donating substituents such as dialkylamino groups. FMO analyses based on the model system calculated by the CNDO/2 method showed that the dominant HOMO–LUMO interaction in the transition state should involve the HOMO of *NN*-dialkylaniline and LUMO of the quinonoid ketene. Thus, the in-plane π*-orbital induces the orthogonal approach of the two components favouring an antarafacial pathway and the cyclisation is initiated by preferential bond formation between the central carbon of the ketene moiety and the *para*-carbon of *NN*-dialkylaniline to result in the formation of (**22**).

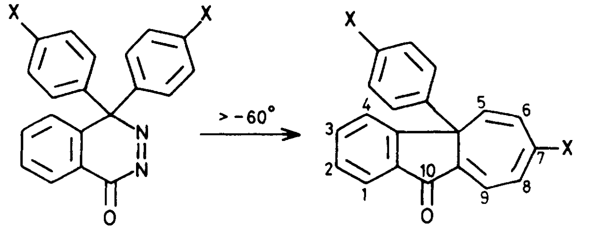

(3b) (14b)

Scheme 1. X = NMe_2

In the preceding paper,[1] we reported the preparation and physicochemical properties of phthalazin-1(4*H*)-one, a six-membered cyclic α-monocarbonyl azo-compound. It was shown that 4,4-diarylphthalazin-1(4*H*)-one derivatives in methylene dichloride solution were stable only below −60 °C and underwent a novel 1,2-aryl migration in strong acid *via* the divalent nitrenium ion, and based on the molecular orbital calculations of the model compound, the electron-donating substituent at C(4) led to an increase in the rate of nitrogen extrusion while electron-withdrawing substituents at the same position substantially stabilised the phthalazin-1(4*H*)-one. A parallel trend was also observed experimentally.

In this paper, we describe what happened when such a solution was warmed to room temperature. The extrusion of molecular nitrogen occurred to result in the formation of a quinonoid ketene. The quinonoid ketene thus generated exhibited quite remarkable behaviour in that it underwent a novel intramolecular cycloaddition with an aromatic ring bearing a *p*-dialkylamino substituent to afford a benzazulenone derivative. We also discuss in detail the mechanism by which the benzazulenone and other products are formed from their various precursors and molecular orbital considerations on the nature of the conjugated ketenes and the regiochemistry of the intramolecular cycloaddition.

Results and Discussion

(1) *Thermal Extrusion of Molecular Nitrogen from Phthalazin-*1(4H)*-one Derivatives* (3) *and Product Identification.*—When a cold CH_2Cl_2 solution containing phthalazin-1(4*H*)-one (**3b**) prepared from the corresponding hydrazide (**2b**) by low-temperature lead tetra-acetate (LTA) oxidation was gradually warmed to room temperature, nitrogen evolution was observed above −50 °C, and the solution displayed colour discharge from deep reddish brown to yellow.

After nitrogen evolution ceased, work-up of the resulting solution gave, in nearly quantitative yield, a single crystalline product, to which we assigned the structure 7-dimethylamino-4b-(*p*-dimethylaminophenyl)benz[*a*]azulen-10-one (**14b**) on the basis of elemental analysis and spectral properties.

Microanalytical and mass spectral data for this product established the molecular formula $C_{24}H_{24}N_2O$. The observed carbonyl stretching frequency (1 655 cm^{-1}) in the i.r. spectrum and intense absorption [$\lambda_{max.}$ 461 nm (log ε 4.41)] in the u.v. spectrum are indicative of an extensively delocalised moiety. Inspection of the n.m.r. spectrum demonstrated the presence of vinyl protons as well as two dimethylamino peaks in magnetically different environments. All these spectral data are consistent with the assigned structure.

The transformation of (**3**) into (**14**) was monitored by i.r. spectral changes as shown in Figure 1. A CH_2Cl_2 solution of (**3b**) at −80 °C exhibited a carbonyl stretching band at 1 715 cm^{-1}. On raising the temperature of this solution, the band due to (**3b**) was gradually replaced by the band due to azulenone (**14b**) at 1 655 cm^{-1}. This indicated that there exists no detectable intermediate along this pathway.

In the light of these observations, one might expect that formation of the azulenone (**14b**) would take place in LTA oxidation even at room temperature. When such an LTA oxidation was carried out using (**2b**) at room temperature under otherwise identical conditions, spontaneous nitrogen evolution occurred. The n.m.r. spectrum of the crude reaction mixture, however, was rather messy and showed the presence of several products. Chromatographic separation afforded five products, which were identified as the azulenone (**14b**), *o*-dibenzoylbenzene derivative (**15b**), the anthrone derivative (**16b**), the anthraquinone derivative (**17b**) and the phthalide (**1b**) in the proportions 3:9:1:1:3.

Compounds (**1b**), (**15b**),[2] and (**17b**)[3] are known and their structures were identified by comparison of m.p., i.r., and n.m.r. data with those of authentic samples. The structure of (**16b**) follows from its spectral properties.

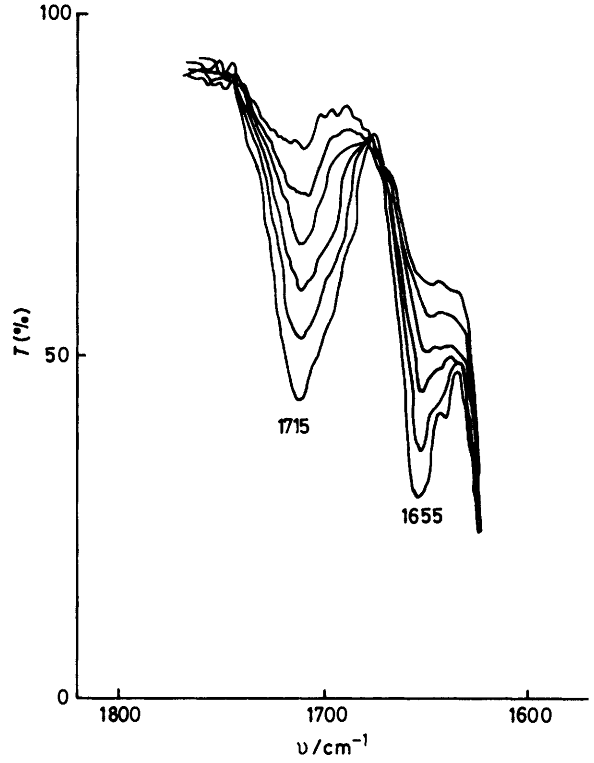

Figure 1. I.r. spectral change of the carbonyl absorption of (**3b**)—(**14b**)

It should be noted that the n.m.r. spectrum of the crude reaction mixture did not show the presence of the anthrone (**16b**) and anthraquinone (**17b**). These products (**16b**) and (**17b**) must have arisen during the column chromatographic separation. In fact, heating a CH_2CH_2 solution of (**14b**) in a sealed n.m.r. tube for 30 min at 80 °C gave (**16b**) quantitatively and leaving this solution to stand in air readily gave (**17b**) nearly quantitatively. These observations reinforced the structural assignment of (**14b**).

(2) *Mechanism of Product Formation.*—On the basis of experimental results described in the previous section, we deduced the following reaction pathway shown in Scheme 3 using compound (**2b**) as an example.

The proposed mechanism by which all five products were formed involves highly reactive intermediates of quinonoid ketene (**19b**) and the norcaradiene derivative (**22b**). The quinonoid ketene (**19b**), was confirmed by trapping with methanol to give methyl *o*-[bis-(*p*-dimethylamino)phenylmethyl]benzoate (**23b**) by adding methanol containing a small amount of sodium methoxide into the reaction mixture at low temperature.

The quinonoid ketene (**19b**) then underwent a regiospecific intramolecular cycloaddition with one of the aromatic rings to give the norcaradiene derivative (**22b**), exclusively. This process can be viewed formally as a thermally allowed $[_{\pi}4_{a} + _{\pi}2_{a}]$ cycloaddition, followed by ring-opening (Cope-type rearrangement) with cleavage of bond a, resulting in the formation of the benzazulenone derivative (**14b**), while a 1,2-hydrogen shift in (**22b**) with cleavage of bond c gave (**16b**).

The formation of (**1b**) and (**15b**) can be interpreted by LTA oxidation of (**22b**), since (**1b**) and (**15b**) would be produced at earlier stages of the reaction due to the instability of (**22b**) at room temperature. In fact, the similar oxidation of (**14b**) at room temperature afforded (**1b**) and (**15b**).

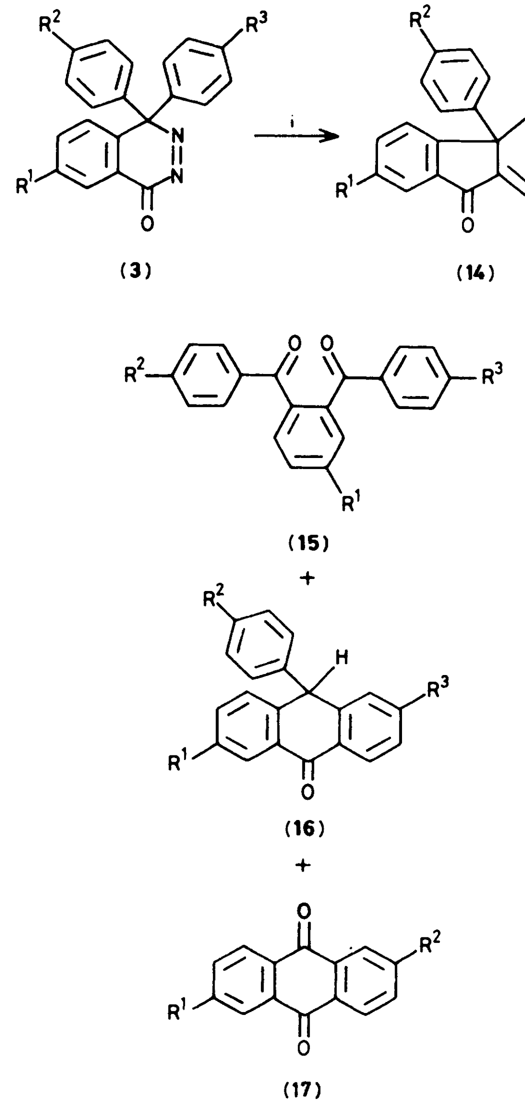

Scheme 2. *Reagents:* i, LTA, room temperature

It should be noted that the formation of (**19b**) is accompanied by disruption of an aromatic ring. Though not directly related to the present case of ground-state chemistry, this is in sharp contrast to light-induced ketene formation from cyclohexadienone, where the quinonoid ketenes are not readily formed from cyclohexadienones 'if net loss of an aromatic sextet is necessary'.[4]

(3) *Thermal Nitrogen Extrusion of Other Phthalazin*-1(4H)-*ones* (**3c**—**g**).—On the basis of the above rationalisation, the cyclisation of the quinonoid ketene (**19**) generated from (**3**) which bears a different substituent at the *para*-position of each 4-aryl ring ($R^2 \neq R^3$) would provide an experimental criterion for the site-selectivity (chemoselectivity) for choosing which aromatic ring preferentially participates in the cyclisation and for the regioselectivity in choosing between the avoidance and preference of an antarafacial pathway.

In fact, LTA oxidation of (**3c**—**g**) at low temperature afforded products whose ratios varied with the *para*-substituent of the 4-aryl ring, and the results are summarised in Table 1.

The structures of these products were established by spectral properties. The formation of (**14**) and (**14′g**) occurred from the

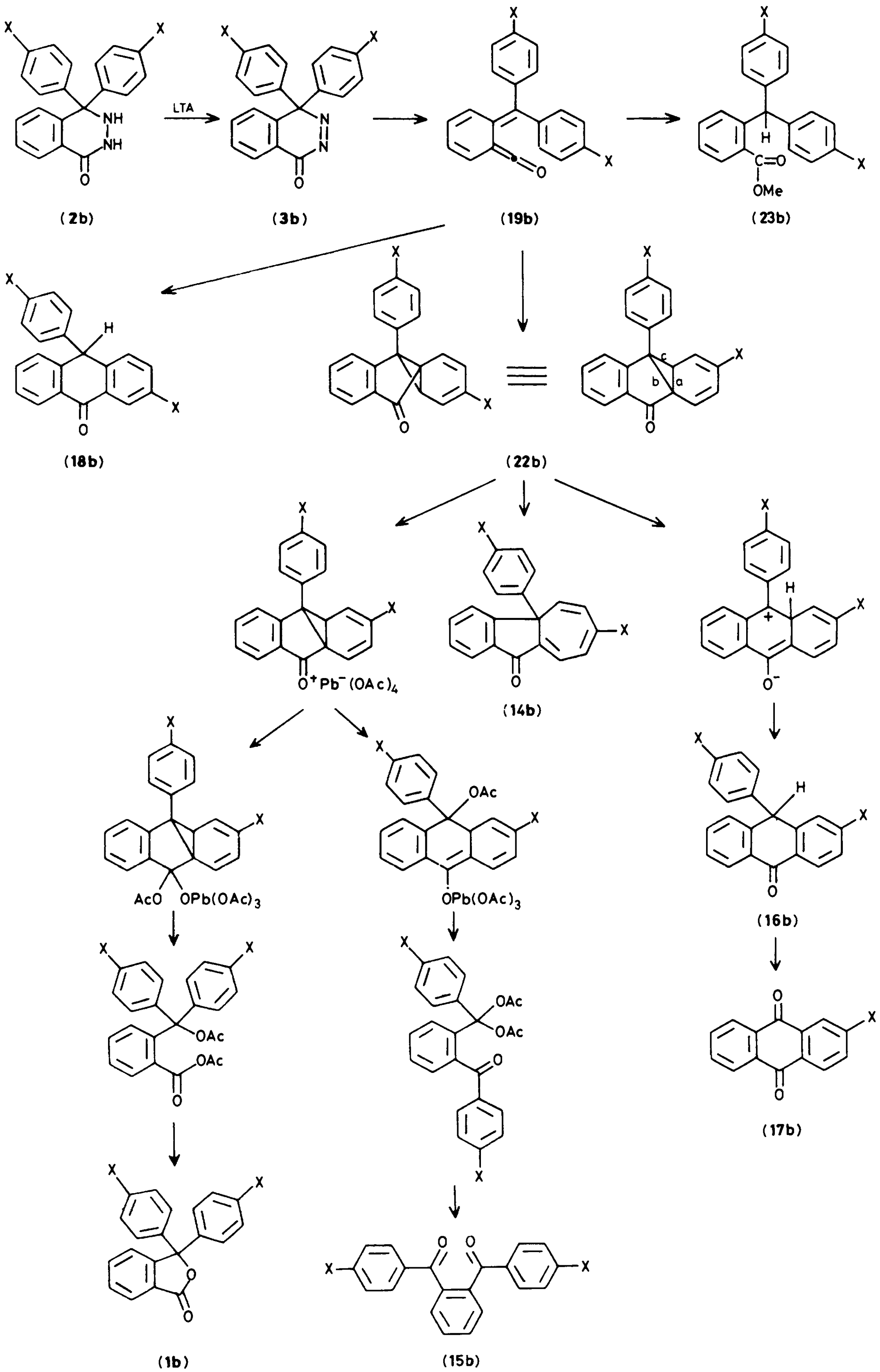

Scheme 3. X = NMe_2

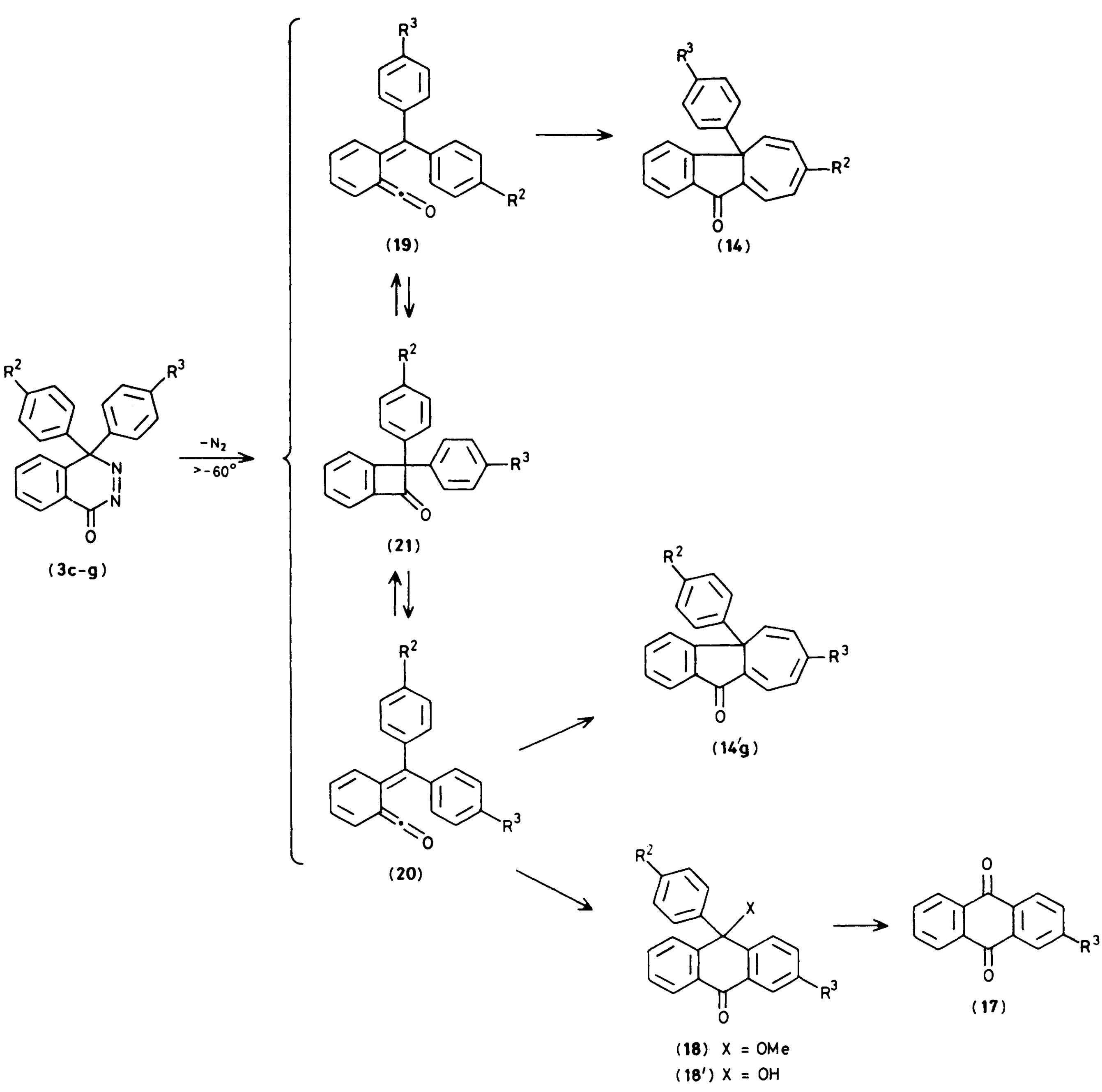

Scheme 4.

Table 1. Product ratio resulting from nitrogen elimination of (3c—g)

	Product ratio (%)				
Compound (3)	(14)	(17)	(18)	(18')	(17) + (24) + (25)
c; R^2 = NMe_2, R^3 = OMe	76.9	17.4	5.7	0	23.1
d; R^2 = NMe_2, R^3 = Me	75.4	6.9	17.7	0	24.5
e; R^2 = NMe_2, R^3 = H	81.5	5.9	12.5	0	18.5
f; R^2 = R^3 = OMe	0	0	8.8	91.2	100.0
g; R^2 = NMe_2, R^3 = NEt_2	100.0[a]	0	0	0	52.5

[a] The ratio between (14g) and (14'g) is 47.5:52.5.

corresponding quinonoid ketene (**19c**) *via* the sequence for (**14b**), while the anthraquinone (**17c**), which is formally obtainable by oxidation from either (**16**) or (**18**), is most probably formed from (**20c**) by 6π-electrocyclisation followed by further oxidation of (**18**) or [(**24**) (**25**)]. Table 1, therefore, implies that the ratio of the participation in cycloaddition is roughly proportional to the magnitude of the electron-donating power of the *para*-substituent and that (**19**) with a *p*-dialkylamino substituent on the 4-aryl ring did undergo regiospecific intramolecular cycloaddition to give the norcaradiene.

(4) *Quantum Chemical Properties of Quinonoid Ketenes and Analysis of the Intramolecular Cycloaddition.*—Although it is already well documented that several linearly conjugated cyclo-

hexadienones photoisomerise to quinonoid ketenes, which undergo intramolecular cycloaddition with an ethylene double bond either to the starting dienones or to bicyclo[3.1.0]hexanones,[5] little notice has been taken of such cycloadditions with an aromatic ring.[6]

Contrary to well investigated ketene cycloadditions,[7] conjugated ketene cycloadditions are poorly understood, despite the fact that intramolecular cycloadditions are often utilised for the synthesis of important classes of cyclic compounds.

In order to provide a fundamental insight into the physicochemical properties of the quinonoid ketenes, and point the way to future experimental designs of the reaction involving such ketenes, we undertook molecular orbital calculations of conjugated ketenes and several molecules relevant to the present discussion by the CNDO/2 method.[8]

The geometries of conjugated ketenes are not known so that planar geometry (C_s symmetry) of the molecules with standard bond lengths and bond angles[9] was assumed.

We also analysed the intramolecular cycloaddition of the quinonoid ketenes in terms of frontier molecular orbital (FMO) theory by separating the quinonoid ketene (**20**) into two moieties, quinonoid ketene (**27**) for the diene segment and monosubstituted benzene for the dienophile segment.[10]

(a) *Molecular orbital properties of conjugated ketenes.* The FMO energies and coefficient distributions of several conjugated ketenes are shown in Figure 2, with those of ketene for comparison.

The coefficients of the HOMO and LUMO clearly show that the carbonyl function of the ketene moiety exerts an influence, similar in nature to that of an electron-donating substituent, on the carbon–carbon π-system, although it plays the role of an electron-withdrawing substituent in the carbonyl π-bonding.

The interesting feature is that the energy level and the coefficient of the in-plane π^*-orbital of the carbonyl group for the conjugated ketene remains essentially unchanged due to orthogonality between the two π-systems. So, the potentiality for orbital interaction would also be unchanged, although the increase in conjugation of the carbon–carbon π-system lowers the unoccupied π-orbital in energy. Consequently, the in-plane π^*-orbital resulted in the NLUMO for (**26**) and (**29**), as opposed to the situation for (**24**) and (**25**), and yet (**27**) underwent reactions by the antarafacial pathway.

(b) *Cycloaddition of the quinonoid ketene with a dialkylanilino group.* The CNDO/2 calculations were performed on several monosubstituted benzenes for comparison with the same level of approximation and the resulting FMO energy diagram is shown in Figure 3. It can be seen that the introduction of a polar substituent perturbs the energy of a b_1-type orbital more than that of an a_2-type orbital and the strongly electron-donating dialkylamino-substituent raises the HOMO energy to a large extent as expected. As a result, the LUMO of the quinonoid ketene (**27**) and the HOMO of dialkylaniline (**31**) and (**32**) have the smaller separation in energy [*e.g.* LUMO (**27**) − HOMO (**31**) = 12.826 eV] compared with the reverse pair [LUMO (**31**) − HOMO (**27**) = 13.512 eV], so that the former may be the dominant orbital pair for determining the regiochemistry of the cycloaddition of (**20**) in FMO terms.

Thus, for intramolecular cycloaddition of the quinonoid ketene with a dimethylanilino group, the planar π^*-orbital, regardless of whether it is LUMO or NLUMO, induces an orthogonal-like approach of each component with charge-transfer stabilisation by the three-centre bond of the central carbon atom with the 2π-component. This type of stabilisation also gives rise to interaction of the 2π-component with the orthogonal p_z orbital of the central carbon atom. Of more importance is the fact that the magnitude of this interaction depends on the magnitude of the interaction between the two p orbitals in the three-centre bonding.

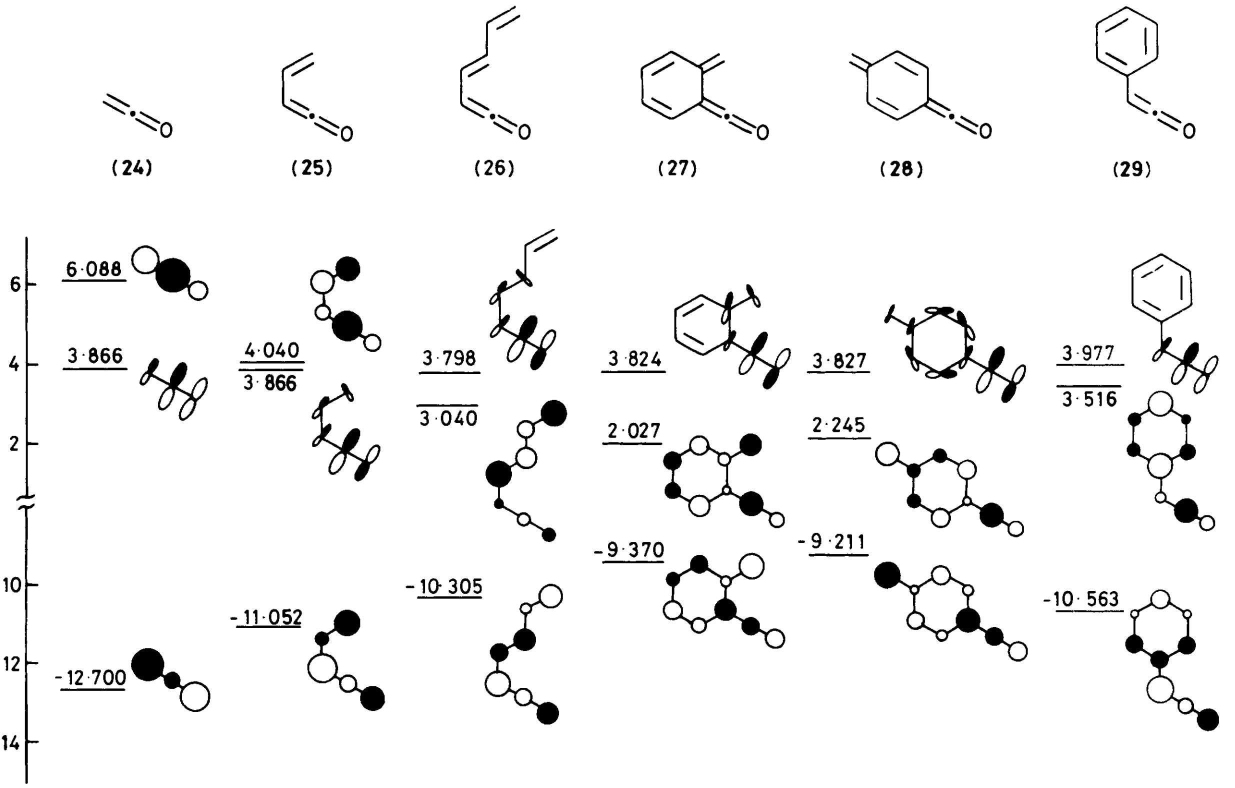

Figure 2. Frontier molecular orbital energies and nodal properties of ketenes (**24**)—(**29**) calculated by the CNDO/2 method

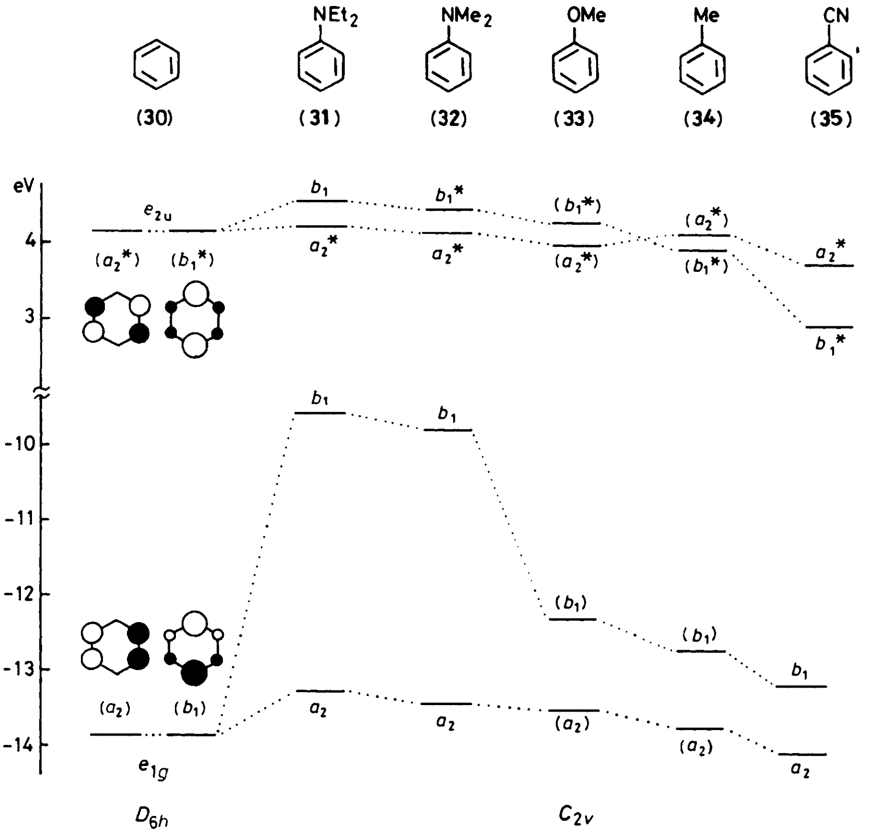

Figure 3. The relative FMO energy diagram of some monosubstituted benzenes calculated by the CNDO/2 method: although introduction of substituents as in (33) and (34) reduces the molecular symmetry to C_s, the point here is in the qualitative nodal properties of the aromatic ring

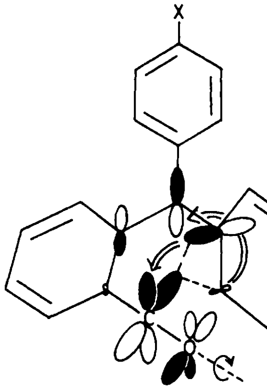

(36)

The novel regiospecific $[{}_{a}4_{\pi} + {}_{a}2_{\pi}]$ intramolecular cycloaddition of (**20a**), therefore, arises from initial bond formation between the central carbon atom of the quinonoid ketene and the carbon atom at the *para*-position of dimethylaniline due to the much greater magnitude of the HOMO coefficient at the *para*-position. This bond formation also brings about concomitant disrotatory motion as in (**36**), leading to the completion of the $[{}_{a}4_{\pi} + {}_{a}2_{\pi}]$ process.

(c) *Cycloaddition of the quinonoid ketene with other monosubstituted aryl derivatives.* The FMO energy separations between the quinonoid ketene (**27**) and several monosubstituted benzenes (**30**)—(**34**) are summarised in Table 2 which clearly indicates that the orbital pair of the smaller FMO energy separation which involves the LUMO of ketenes (**27**) and the HOMO of aromatic derivatives (**30**)—(**34**) only applies to dialkylanilines (**31**) and (**32**). This is obviously because the HOMO energies of the other monosubstituted benzenes except dialkylanilines are much lower than those of dialkylanilines (**31**) and (**32**) as shown in Figure 3. Therefore, there is little interaction of the 2π-component with the in-plane π^*-orbital of the quinonoid ketene and the dominant orbital interaction in the transition state of the intramolecular cycloaddition of (**20**) with monosubstituted benzenes other than dialkylaniline in between the HOMO of the quinonoid ketene and the LUMO of the monosubstituted benzene in FMO terms. The NLUMO energy of the monosubstituted benzenes is close to that of the LUMO and its interaction in the transition state with the HOMO of the quinonoid ketene should also be large. Consequently, the magnitude of the LUMO coefficient would not appreciably affect the regiochemistry of the intramolecular cycloaddition.

Table 2. FMO energy separation (eV) between quinonoid ketene (**27**) and some monosubstituted benzenes (**30**)—(**34**)

Monosubstituted benzene	$\text{LUMO}_{\text{ketene}} - \text{HOMO}_{\text{aromatic}}$	$\text{LUMO}_{\text{aromatic}} - \text{HOMO}_{\text{ketene}}$
Diethylaniline	*12.628*	13.574
Dimethylaniline	*12.826*	13.512
Anisole	14.362	*13.346*
Toluene	14.762	*13.304*
Benzene	15.896	*13.513*

Thus, the quinonoid ketene (**21**) undergoes a normal 6π-electrocyclisation in accord with the experimental facts. Experi-

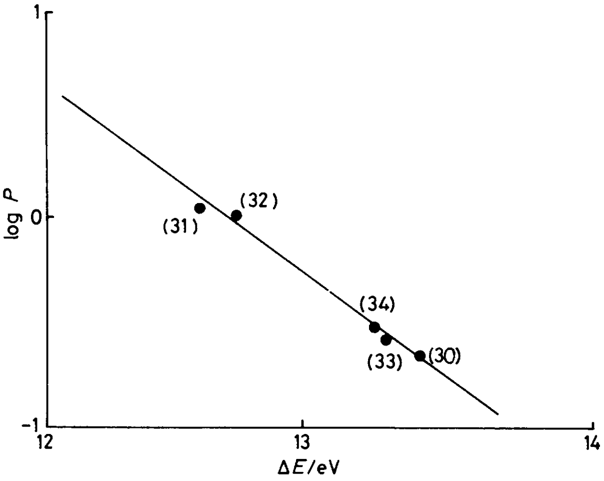

Figure 4. The plot of log P *versus* HOMO − LUMO energy separation (ΔE).

mental and theoretical studies of this type of cycloaddition show that the antarafacial pathway of the quinonoid ketene reported herein can occur only when the aromatic ring possesses a strong electron-donating substituent such as a dialkylamino group.

Furthermore, these results provided additional insight into the nature of the quinonoid ketene. The experimental results in Table 1, combined with the results in Table 2, revealed that the product ratio (P) derived from cyclisation with the dimethylanilino group is proportional to the orbital pair of the smaller FMO energy separation between the quinonoid ketene (**27**) and the aromatic segment (shown in italics in Table 2).

A plot of log P as a function of the orbital pair of the smaller HOMO − LUMO energy separation shows a linear relation, despite the difference in the cyclisation pathway (Figure 4).

These results are strongly suggestive of rapid equilibrium between the two quinonoid ketenes (**19**) and (**20**), which most likely occurs *via* the benzocyclobutenone (**21**).

References

1 M. Kuzuya, F. Miyake, and T. Okuda, preceding paper.
2 Guyot and Haller, *Ann. Chim. Phys.*, 1881, **19**, 341.
3 J. Limpricht, *Ann. Chem.*, 1899, 305, 307.
4 M. Miller and A. K. Bhattacharya, *Tetrahedron Lett.*, 1981, **22**, 3757.
5 (*a*) D. H. R. Barton and G. Quinkert, *J. Chem. Soc.*, 1960, 1; (*b*) G. Quinkert, *Angew. Chem., Int. Ed. Engl.*, 1965, **4**, 211; (*c*) O. L. Chapman and J. D. Lassila, *J. Am. Chem. Soc.*, 1968, **90**, 2449; (*d*) J. Griffithes and H. Hart, *ibid.*, p. 3297; (*e*) M. R. Morris and A. J. Waring, *Chem. Commun.*, 1969, 526; (*f*) G. Quinkert, B. Bronstert, D. Egert, P. Michaelis, P. Jürges, G. Prescher, A. Syldatk, and H.-H. Perkampus, *Chem. Ber.*, 1976, **109**, 1332; (*g*) for a recent review, see G. Quinkert, *Angew. Chem.. Int. Ed. Engl.*, 1975, **14**, 790.
6 (*a*) J. Rigaudy and N. Pailloud, *Tetrahedron Lett.*, 1966, 583; for the closely related ketene imine case, (*b*) E. M. Birges and G. Milne, *ibid.*, p. 93; (*c*) G. Ege, *Chem. Ber.*, 1968, **101**, 3079.
7 (*a*) R. B. Woodward and R. Hoffmann, 'The Conservation of Orbital Symmetry,' Academic Press, New York, 1970, p. 163; (*b*) I. Fleming, 'Frontier Orbitals and Organic Chemical Reactions,' Wiley-Interscience, London, 1976, p. 143. For an alternative treatment of ketene addition to olefins, see H. E. Zimmerman, *Acc. Chem. Res.*, 1971, **4**, 272.
8 (*a*) J. A. Pople, D. P. Santry, and G. A. Segal, *J. Chem. Phys.*, 1965, **43**, 129; (*b*) J. A. Pople and G. A. Segal, *ibid.*, p. 136.
9 J. A. Pople and D. L. Beveridge, 'Approximate Molecular Orbital Theory,' McGraw Hill, New York, 1970, p. 111.
10 (*a*) K. Fukui and H. Fujimoto, 'Mechanisms of Molecular Migrations,' ed. B. S. Thyagarajan, Interscience, New York, 1969, vol. 2, p. 117; (*b*) K. Fukui, *Acc. Chem. Res.*, 1971, **4**, 57.

Received 30*th September* 1983; *Paper* 3/1727